International Journal of Technical Innovation in Modern Engineering & Science (IJTIMES)
Impact Factor: 5.22 (SJIF-2017), e-ISSN: 2455-2585
Volume 5, Issue 06, June-2019

Three phase battery storage system for distribution grid application

Dhiraj Dattatraya Chaudhari[1], Prof. A P Chaudhari[2]

[1]*Hindi Seva Mandal's Shri Sant Gadge Baba College of Engineering & Technology*
[2]*Hindi Seva Mandal's Shri Sant Gadge Baba College of Engineering & Technology*

Abstract— In this paper we have explained, the H Bridge topology configuration meets many stipulations in the Industry of Power Electronics with the closer progress in MOSFET switches the cost, size and installation area are highly lay off. It is a transformer less process in order to increase the quality of the Power with reduction in losses and stress. In the PV panel the solar radiance method is employed for energy harvesting in Agriculture site. Finally, the simulation relations using MATLAB / Simulink show the suitability and execution of the suggested model in PV storage system for the prediction of Boosted PV output power

Index words: H - bridge multilevel inverters, Photovoltaic module, Invertor, MATLAB.

INTRODUCTION

Environmental concern and the required to find cleaner energy sources have concluded in the fast-increasing saturation of formation and circulation sector from renewable resources like solar power sources. But as infiltration of variable generation sources reaches and rise above the 10–30% range, equivalent supply to load will begin to counterfeit a important confront. With such transformations frightening in the future, energy storage will become vital to creating a power system that can handle both the changeability and unpredictability of renewable resources in an increasingly complex and assorted grid. The controlling and coordinating BES units in a PV storage system for smoothing the intermittency of the solar resource and changing output to more closely match the load side view. The PV storage system is modelled as turned in optimization problem and Model Predictive Control (MPC) structure solves the optimization problem using external price signals and predictions of PV output at each time step. Our computation consists of an asymmetric least square fit of the PV output data with a linear error correction to handle uncertainties and provide forecasts to enable dynamic power forecast. Energy harvesting from ambient energy sources together with sunlight, wind, and tidal wave can present unrestrained and unlimited power supply for entrenched systems. However, the harvested energy exhibits intermittency characteristics. For instance, the output power of a photovoltaic (PV) panel at noon is an order of scale higher than that in the morning or evening.

LITERATURE SURVEY

In the last some years, so many multilevel inverter structures have been recommended for accomplishing high output voltage and power. Multi-level inverters are basically designed to generate low- cost power and used in grid-connection applications at different levels of voltage because in most cases it is hard to connect a individual power semiconductor shift directly to the gird. Such technologies also reduce total harmonic distortion (THD %), dv/dt, and electromagnetic interference. Multi-level inverter topologies can be grouped into common dc-link, cascaded separate dc sources, isolated topologies, and interconnected three-phase inverters. Further, some more types of topologies have also come up such as the one carry put by means of descend elemental cell structures called hybrid inverters. However, some of those topologies combine more than one fundamental converter or conventional cascaded multi-level structure.

Common dc-link multilevel converters, such as diode-clamped or Neutral Point Clamped (NPC) converter, capacitor-clamped or Flying Capacitor (FC) inverter, and Modular Multilevel converter (MMC), were proposed for high power applications. In an NPC inverter, capacitors are connected in series to share the voltage where diodes are used to clamp voltages across capacitors. As a conclusion, each switch holds with only one capacitor voltage. However, the inverter suffers from capacitor unbalance voltage issue and unfavourably big number of clamping diodes when the number of voltage level is large.

Reversal reconstruction of clamping diodes is one more design flaw when the inverter is controlled under PWM - Pulse Width Modulation techniques. Capacitors, in a waving inverter, are employed to clamp voltage beyond switches. It is comparable to a diode-clamped inverter but with more capacitors. furthermore, this type of inverter needs problematic control approach to regulate the waving capacitor voltages. furthermore, the MMC topology is a common dc- link but with a cascaded multilevel structure where the converter is represented by a modular arm with upper/lower legs composed of series connection of power converter modules. The advantages of high modularity and voltage scalability allow this structure to be connected directly to grid with no need of transformer. Capacitor voltage readjusting is plain

compared to other normal dc-link multi-level converters, which makes the modular multi-level converter effective in multiple applications. Huge inductors are a must for an MMC converter to regulate the flow of current due to the changeable voltage over the arm inductor. Some other issue is the count of capacitors. After all, all battery modules/cells in the earlier frequent dc-link multilevel converters have a frequent dc link where all system battery bunch are interconnected in parallel and series, thereby sharing the total power. Such converter topologies are not enticing for huge energy storage systems when we need power management and balancing on each battery module/cell.

In this argumentation work, two new more cascaded multilevel inverter topologies are represented to accommodate and manage grid-level battery energy storage systems. Another one developed converter, the Six-Switch Cascaded Transformer (SSCT) multilevel converter, is distinct from the conventional isolated cascaded H-bridge multilevel inverter, which has only one battery packs string. The another more recommended multilevel inverter is a hierarchical-cascaded multi-level inverter with the ability to complete uniform state of charge action and removal power between battery strings (phases) of the three-phase BESS system.

SYSTEM ARCHITECTURE

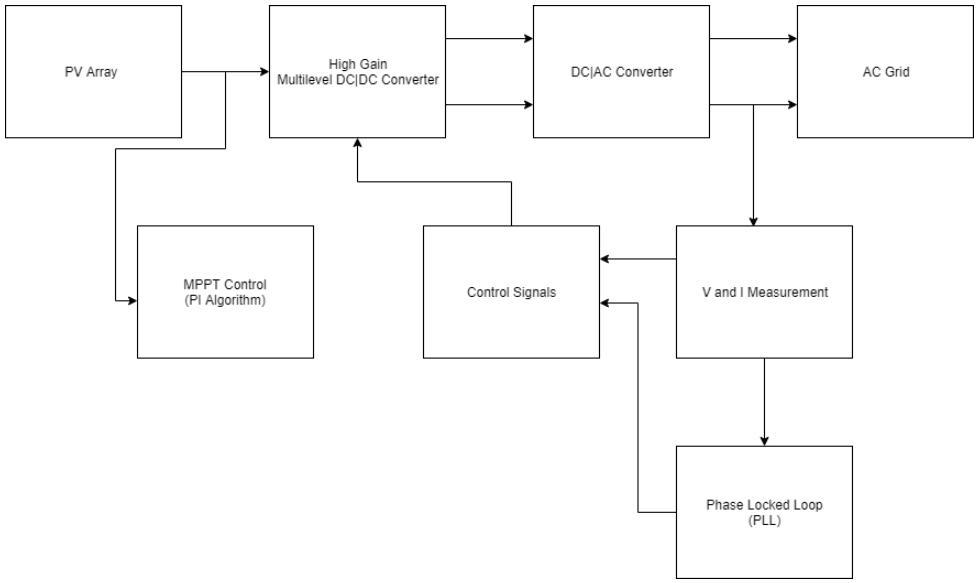

Fig 1. System Architecture

Battery storage system Fig. 2 presents a simplified single-line diagram of a medium voltage distribution system with the BSS. The grid is composed of the main generation, distribution transformers, four feeders, linear and non-linear load and passive filters. The BSS is connected to the PCC4. Fig. 3 presents the single-line diagram of the BSS. The BSS contains eight H-bridge converters. Each converter has a bank of battery with 75 12 V/600 Ah batteries, represented by Vdc. The output filter is composed only of an inductor. The BSS current and the PCC4 voltage are the variables used in the control strategy. The batteries currents are used to estimate their SOC. A bypass switch is represented at the lower converter in order to emulate a failure.

Control strategy

Fig. 3 shows the control strategy block diagram. The diagram is for phase A, but it is valid also for phases Band C. A phase-locked loop is used in order to obtain a synchronised sinusoidal reference related to the PCC4 voltage. The power references for charging (Pref charge) and for discharging (Pre-discharging) are used to charge and discharge the batteries. For the charging process, the power reference is limited to the BSS power rate. For discharging, the BSS can realise this process at its battery capacity rate or the system operator can define the amount of active power to be injected into the grid. The SOC evaluation decides if the BSS is set to charge or discharge the batteries. Information about the PCC4 reactive energy is obtained through the conservative power theory and it is added to the BSS reference if the system operator wants power quality improvement in PCC4. The current control loop block is a closed-loop mesh that controls the BSS output current.

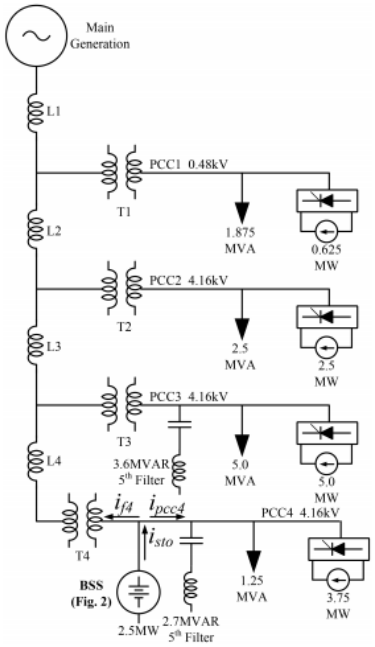

Figure 2 Simplified single-phase diagram of a medium-voltage distribution

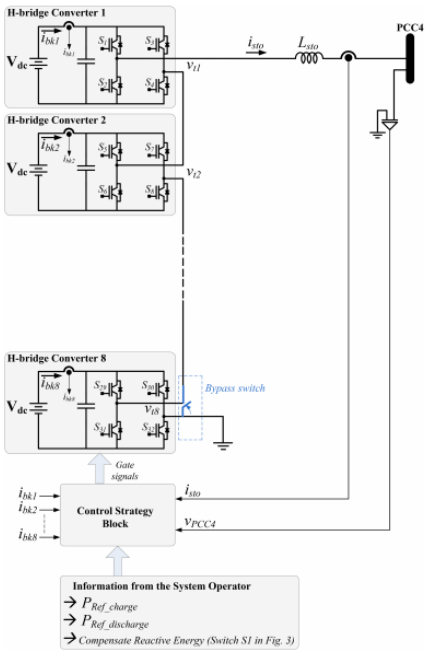

Fig 3 Single-line diagram of the BSS

The current control loop guarantees that the BSS output current follows its reference signal independent of its waveform. Fig. 3.4 presents the current control loop block diagram. The measured current (Isto) is subtracted from the current reference (Isto*) and the resulted error signal (e) is sent to the controller, which, in turn, acts on the CHB through the modulated signal (u). A voltage feed forward (vPCC4) is added to the current controller output signal. The CHB plus the output filter is represented by a current plant (G(s)). The current sensor gain is assumed to be unitary. The control objective can be expressed in mathematical form as

$$istot \rightarrow isto* \text{ t as } t \rightarrow \infty \quad (1)$$

To guarantee (1), the system must be mathematically modelled. The model can be obtained by a simple application of Kirchhoff's laws at PCC4. This yields the following model that describes the system dynamics.

$$L_{sto}\frac{di_{sto}(t)}{dt} = v_t(t) - v_{PCC4}(t) \quad (2)$$

$$L_{sto}\frac{di_{sto}(t)}{dt} = \sum_{i=1}^{8} v_{ti} - v_{PCC4}(t) \quad (3)$$

$$i_{sto}(t) = i_{f4}(t) + i_{pcc4}(t) \quad (4)$$

The H-bridge converter terminal voltages can be written as

$$\begin{bmatrix} v_{t1}(t) \\ v_{t2}(t) \\ v_{t3}(t) \\ v_{t4}(t) \\ v_{t5}(t) \\ v_{t6}(t) \\ v_{t7}(t) \\ v_{t8}(t) \end{bmatrix} = \begin{bmatrix} u_1(t)V_{dc} \\ u_2(t)V_{dc} \\ u_3(t)V_{dc} \\ u_4(t)V_{dc} \\ u_5(t)V_{dc} \\ u_6(t)V_{dc} \\ u_7(t)V_{dc} \\ u_8(t)V_{dc} \end{bmatrix} \quad (5)$$

where u1, u2 …… u7, u8 denote the modulation signals for each H-bridge converter. Their signals are continuous, and their values are in the range [−1;1]. To facilitate the controller design and to reduce the model expressions, it is convenient to transform (5) by the definition given in the following equation:

$$\lambda(t) = u_1(t) = u_2(t) = u_3(t) = u_4(t) = u_5(t) = u_6(t) = u_7(t) = u_8(t) \quad (6)$$

Therefore, (3) can be rewritten as

$$L_{sto}\frac{di_{sto}(t)}{dt} = 8V_{dc}\lambda(t) - v_{PCC4}(t) \quad (7)$$

The last term can be considered as disturbance and may be omitted. By applying the perturbation and linearization technique and taking the Laplace transformation, the CHB plus output filter transfer function (G) is given as

$$G(s)\frac{I_{sto}(s)}{\lambda(s)} = \frac{8V_{dc}}{sL_{sto}} \quad (8)$$

The PWM transfer function is given by (9), where vtp is the peak value of the triangular carrier and its value is equal to one

$$\mathrm{PWM}(s) = \frac{1}{v_{tp}} \quad (9)$$

The proportional–integral (PI) controller transfer function is given as

$$C(s) = \frac{\lambda(s)}{e(s)} = \frac{k_p(sT_{PI}+1)}{sT_{PI}} \quad (10)$$

The closed-loop transfer function that relates the CHB output current and its reference is given as

$$\frac{I_{sto}(s)}{I_{sto}*(s)} = \frac{8V_{dc}k_p(sT_{PI}+1)}{s^2T_{PI}L_{sto} + s8V_{dc}k_pT_{PI} + 8V_{dc}k_p} \quad (11)$$

Omitting the one-sampling delay, the damping factor is given as

$$\xi = \frac{1}{2}\sqrt{\frac{8V_{dc}k_pT_{PI}}{L_{sto}}} \quad (12)$$

$\xi = 1$ leads to a critical damping response. Moreover, the time constant TPI must be assigned to be much longer than the control delay from the viewpoint of control stability.

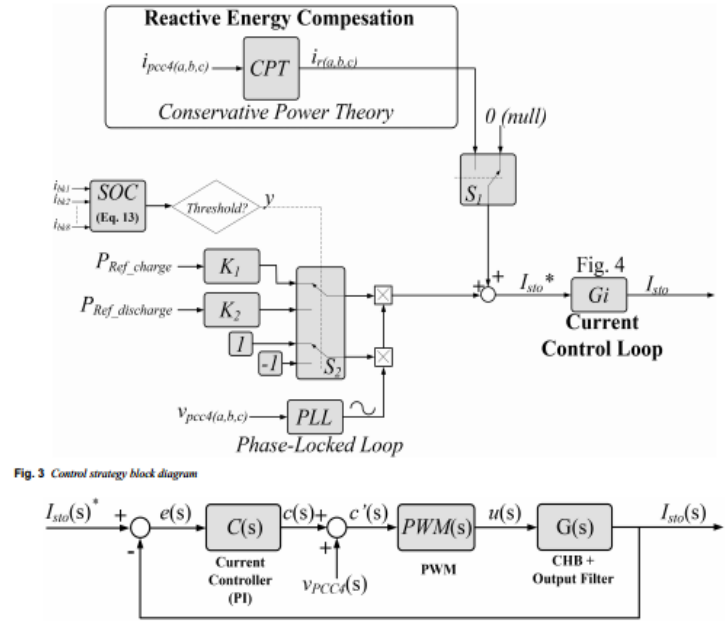

Fig. 3 *Control strategy block diagram*

Fig 4 Control strategy block diagram

Estimating the SOC and state-of-health (SOH)

Applications covering batteries usually use a model in order to describe their behaviour. The model may contain parameters like SOC, SOH, terminal voltage, cell temperature and internal pressure. The battery SOC is not directly measured and estimation must be done. A simplified way to estimate the SOC is given as

$$SOC(t) = 100\left(\frac{Q_{nom} - \int_{\tau_0}^{\tau} i_{bat}(t)dt}{Q_{nom}}\right) \quad (13)$$

where Q nom and I bat are the battery nominal charge and the instantaneous current, respectively. In the proposed BSS, the SOC is measured for the average current of all batteries. Moreover, the charge and discharge process are assumed to be the same for all banks. The BSS proposed in this paper considers that the battery is fully charged and discharged when its SOC is 95 and 40%, respectively. These values are used in the SOC inquiry of the control strategy. The choice of these values is based on the spinning reserve criteria, which allow the BSS to compensate unpredictable imbalances between the load and generation caused by sudden outages of generating units. On the other hand, the SOH is a measurement used to qualify the battery condition. The SOH states the age and degradation

Table 1 System parameters used in the simulation

Parameter	Value
main generation RMS voltage	V_g = 13.8 kV
PCC4 RMS voltage	V_{pcc4} = 4.16 kV
system frequency	f_g = 60 Hz
BSS nominal power	P_{BSS} = 2.5 MW
V_{dc} voltage for each converter	V_{dc} = 75 × 12 V/600 Ah
BSS output inductance	L_{sto} = 1000 μH
PI time constant	T_P = 15 ms
sampling frequency	F_s = 30 kHz
switching frequency for each H-bridge converter	F_{sw} = 600 Hz
damping factor	ξ = 1
PI time constant (adopted)	T_{PI} = 20 ms

Table 2 THD for phases *A*, *B* and *C* for the simulated results

THD	Value, %
phase *A*	2.09
phase *B*	1.94
phase *C*	2.38

of a battery and may be estimated by means of verifying one of the following behaviours: increased float current, increased battery impedance, high cell voltage variation, reduced ability to receive a charge and the counting of the number of cycles. Counting the number of cycles is an attractive manner to evaluate the SOH. A high value is indicative of an old battery. Therefore, each charging cycle is counted, and its value is sent to a system operator, which in turn, can use such data to plan the energy delivery and maintenance.

CONCLUSION

This paper represents a three-phase BSS with a transformer less cascaded multilevel inverter for dissemination grid applications. The BSS is composed of eight series-connected H-bridge converters, making it unnecessary to use any bulk transformer. Each converter contains a battery bank made up of 75 12 V/600Ah lead-acid batteries. The BSS is also able to keep working even if one of its converters fails. furthermore, reactive energy compensation is also performed by the proposed BSS. A case study with simulated and experimental results in HIL system shows the performance of the BSS to be excellent. The charging and discharging processes result in sinusoidal currents that are in-phase with the voltages at the point of common coupling, PCC4. In both cases, the power distribution among the converter is always linear, showing an equal-power processing. A failure in one of the H-bridge converters is emulated and the results demonstrate that the BSS kept working uninterrupted. Therefore, the proposed BSS is an attractive solution for applications in medium-voltage grids, contributing to the reliability and to the uninterrupted supply of the distribution system. Moreover, new functions can be embedded in the proposed BSS without the necessity of changing the physical structure. This increases the options of management of the system operator.

REFERENCES

[1] R. Raud, R. Jacob, F. Bruno, G. Will, and A. Steinberg, "A critical review of eutectic salt property prediction for latent heat energy storage systems," Renewable and Sustainable Energy Reviews, vol. 70, pp. 936-944, 2017.

[2] C. Haisheng, C. Thang Ngoc, Y. Wei, T. Chunqing, Y. Li, and D. Yulong, "Progress in electrical energy storage system: A critical review," Progress in Natural Science 19, pp. 291–312, 2009.

[3] H. Ibrahim, I. Adrian, and P. Jean, "Energy storage systems characteristics and comparisons," Renewable and sustainable energy reviews 12.5, 1221-1250, 2008.

[4] F. Di´az-Gonza´lez, A. Sumper, O. Gomis-Bellmunt, and R. Villafa´fila-Robles, "A review of energy storage technologies for wind power applications," Renewable and Sustainable Energy Reviews, vol. 16, no. 4, pp. 2154-71, May 2012.

[5] J.M. Carrasco, L.G. Franquelo, J.T. Bialasiewicz, E. Galvan, R.C.P. Guisado, Ma.A.M. Prats, J.I. Leon, and N. Moreno-Alfonso, "Power-electronic systems for the grid integration of renewable energy sources: a survey," IEEE Trans. on Industrial Electronics, vol. 53, no. 4, p 1002-16, June 2006.

[6] A. Khaligh, Z. Li, "Battery, Ultracapacitor, Fuel Cell, and Hybrid Energy Storage Systems for Electric, Hybrid Electric, Fuel Cell, and Plug-in Hybrid Electric Vehicles: State of the Art," IEEE Trans. on Vehicular Technology, vol. 59, no. 6, pp. 2806-14, July 2010.

[7] C. Jian, and A. Emadi, "A new battery/ultracapacitor hybrid energy storage system for electric, hybrid, and plug-in hybrid electric vehicles," IEEE Trans. on Power Electronics, vol. 27, no. 1, pp. 122-32, Jan. 2012.

[8] A. Emadi, S.S. Williamson, and A. Khaligh, "Power electronics intensive solutions for advanced electric, hybrid electric, and fuel cell vehicular power systems," IEEE Trans. on Power Electronics, vol. 21, no. 3, pp. 567-77, May 2006.

[9] A. Dekka, R. Ghaffari, B. Venkatesh, and W. Bin, "A survey on energy storage technologies in power systems," IEEE Electrical Power and Energy Conference (EPEC), pp. 105-11, 2015.

[10] K. Panagiotou, C. Klumpner, and M. Sumner, "The effect of including power converter losses when modelling energy storage systems: A UK domestic study," 18th European Conference on Power Electronics and Applications, October 25, 2016.